Hyperfine Interact
DOI 10.1007/s10751-015-1160-x

Mössbauer and Raman spectroscopy characterization of concretes used in the conditioning of spent radioactive sources

F. Monroy-Guzman[1] · M. González-Neri[1,2] · R. C. González-Díaz[1] · G. Ortíz-Arcivar[1] · I. J. Corona-Pérez[1] · N. Nava[3] · A. Cabral-Prieto[1] · L. Escobar-Alarcón[1]

Abstract Spent radioactive sources are considered a type of radioactive waste which must be stored properly. These sources are usually conditioned in concrete that functions as shield and physical barrier to prevent the potential migration of radionuclides, and must have suitable properties: mechanical, thermal or irradiation resistance. Concretes used in the conditioning of spent radioactive source in Mexico were tested, preparing concrete test specimens with Portland cement CPC 30RS EXTRA CEMEX and aggregates, and subjected to compression strength, γ-ray-irradiation and thermal resistance assays and subsequently analyzed by Mössbauer and Raman Spectroscopies as well as by Scanning Electron Microscopy, in order to correlate the radiation and temperature effects on the compressive strengths, the oxidation states of iron and the structural features of the concrete. Iron was found in the concrete in Fe^{2+} and Fe^{3+} in the tetrahedral (T) and two octahedral positions (O1, O2). Radiolysis of water causes the dehydratation (200-600 kGy) and rehydratation (1000-10000 kGy) of calcium silicate hydrates (C-S-H) and ferric hydrate phases in concretes and structural distortion around the iron sites in concretes. The compressive strength of concretes are not significantly affected by γ-radiation or heat.

Proceedings of the 14th Latin American Conference on the Applications of the Mössbauer Effect (LACAME 2014), Toluca, Mexico, 10-14 November 2014

✉ F. Monroy-Guzman
fabiola.monroy@inin.gob.mx

[1] Instituto Nacional de Investigaciones Nucleares. Carretera México-Toluca s/n, La Marquesa, Ocoyoacac, Edo. de México, C. P. 52750, México

[2] Universidad Mexiquense del Bicentenario Unidad Lerma, Parque Industrial Automotriz Ex Hacienda Doña Rosa, Lerma Edo. México México

[3] Instituto Mexicano del Petroleo, México City, México

Published online: 27 March 2015

Keywords Concretes · Radioactive sources · Mössbauer · Raman · SEM

1 Introduction

Sealed radioactive sources are extensively used in industry, medicine and agriculture. These sources are permanently sealed in a capsule or bonded in a solid form in order to prevent the spread of radioactive material. At the end of its useful life, these sources are considered ”spent” or ”disused”, however, the residual radioactivity levels of some sources may be high representing a significant radiological hazard. Hence, spent sealed radioactive sources are considered a type of radioactive waste that must be stored properly to ensure its integrity and prevent or limit the release of radionuclides to the environment and to protect people. The spent sealed radioactive sources can be conditioned in concrete which meets two main functions: 1) shield radioactive source for its safe handling, transportation, storage or disposal, and 2) serve as physical barrier to reduce the potential migration of radionuclides during its storage or disposal [1] Thus, these concretes must have specific desired properties (mechanical, thermal or radiation resistance) that assure an adequate handling, transportation, storage or disposal of these sources.

Around 8189 spent sealed radioactive sources (Am-241, Ir-192, Ra-226, Cs-137, Co-60, Sr-90, Po-210, Th-230, etc.), generated in Mexico, have been immobilized in concrete. The concretes used in the conditioning of these sources have not yet been standardized and characterized, however they have to comply with the NOM-0019-NUCL-1995 standard [1, 2]. Therefore, concrete specimens prepared following the formulation used for the conditioning of these sources (from Portland cement: CPC 30RS EXTRA CEMEX manufactured in Mexico) were tested and subjected to compression strength, γ-ray irradiation and thermal resistance assays, in order to correlate the radiation and temperature effects on the compressive strengths, the oxidation states of iron and the structural features of the concrete.

2 Methodology

2.1 Samples preparation

Concrete test specimens, cylinders of 4.5 cm diameter and 7.5 cm length, were prepared by the following formulation: 24.6 % Portland cement CPC 30RS EXTRA CEMEX, 29.5 % coarse aggregates (gravel), 24.6 % fine aggregates (sand) and 21.3 % water. After the 28 days curing time, concrete specimens and raw materials were subjected to compression strength, γ-ray irradiation and thermal resistance assays.

2.2 Compression tests

The compression testing was performed on a MTS 810 Servo-hydraulic test machine, following the ASTM C-39 standard procedure, 2.5 mm/min [3].

2.3 γ-ray irradiation

Concrete test specimens were γ-ray irradiated using doses of 100, 200, 400, 600, 1000 and 10000 kGy with a Co-60 source at the Gamma Irradiator JS-6500.

2.4 Thermal treatments

For the thermal testing, concrete specimens were placed in a chamber with humidity and temperature controlled conditions, and stabilized at 20 °C and 65 % humidity. Subsequently specimens were introduced in a thermal test chamber which was programmed to perform the following thermal cycle, which was repeated five times: (a) starting at 20 °C, the temperature was lowered to -20 °C at a cooling rate of 10 °C/h maintaining the temperature at - 20 °C for 24 hours and subsequently (b) the temperature was raised to 40 °C at a heating rate of 10 °C/h maintaining the temperature at 40 °C for 24 hours. When the fifth cycle was completed, the temperature was raised lowered to 20 °C at a rate of 10 °C/h.

2.5 Characterization

Raw materials, untreated and treated concrete specimens were analyzed by Raman Spectroscopy (RS) Scanning Electron Microscopy (SEM) and Mössbauer Spectroscopy (MS).

RS was performed by using a high resolution micro-Raman system, Horiba Jovin Yvon model LabRAM 800. A Nd:YAG laser beam (532 nm) was focused by a 50X microscope objective on the sample surface. Raman spectra were acquired from 200 to 1800 cm^{-1} at a spectral resolution of about 2 $cm.^{-1}$ A cooled CCD camera was used to record the spectra, varying the acquisition time from 5 to 20 s, usually averaged for 50 accumulations in order to improve the signal to noise ratio. All spectra were calibrated using the 521 cm^{-1} line of silicon and corrected by background subtraction. Multiple spot analyses on different areas of the samples were performed to ensure representative results.

The morphology of concretes was observed from SEM micrographs obtained with a JSM-0009 Scanning Electron Microscope. Digital images were obtained at 100X, 500X, 1000X, 2000X and 5000X magnifications in randomly selected areas.

Transmission Mössbauer spectra were recorded at 300 K by using a conventional constant acceleration spectrometer (Wissel), which was equipped with a krypton proportional detector. The γ-ray source was a ^{57}Co source of 925 MBq (25 mCi) diffused within a rhodium matrix. The isomer shift data are given relative to that of α-Fe. The transmission spectra were numerically analyzed by using the NORMOS program.

3 Results

The γ-ray irradiation and thermal treatments applied to the concrete specimens mostly cause a slight decrease of its compression strength (2-5%), except for the case of the concrete γ-ray irradiated at 1000 kGy which decreased around 13 % (See Table 1). Therefore, the effect of both treatments on the mechanical properties of the concrete is minimal. The compressive strengths of all concrete test specimens were between 30 and 50 times higher than the required by the NOM- 0019-NUCL-1995, (>0.35 MPa) as shown in Table 1.

3.1 Raman spectroscopy

Concrete is formed by combining Portland cement, water and aggregates (sand and gravel). Cements consist of four main solid phases namely: Tricalcium Silicate Ca_3SiO_5 (C_3S),

Table 1 Compression strength of concrete test specimens

Sample Irradiation (kGy)	Compression strength (MPa)
0	36.8 ±2.7
200	34.8 ±1.1
400	34.7 ±2.2
600	36 ±3.5
1000	32 ±4.2
10000	34 ±2.6
Thermal	34.8 ±1
NORME	0.35

Dicalcium Silicate Ca_2SiO_4 (C_2S), Tricalcium aluminate $Ca_3Al_2O_6$ (C_3A) and TetracalciumAlumino Ferrite $4CaO{\bullet}Al_2O_3{\bullet}Fe_2O_3$ (C_4AF). During the formation of concrete, Calcium Silicate Hydrate (C-S-H) gel (torbermorite) and calcium hydroxide ($Ca(OH)_2$ (portlandite)) are formed from the silicates phases, whilst Calcium trisulfoaluminate hydrate: ettringite $3CaO{\cdot}\ Al_2O_3{\cdot}\ 3CaSO_4{\cdot}\ 32H_2O$(E) and monosulfoaluminate hydrate (S) or monosulfoferric hydrate are formed from aluminate phases [4]. The physical and mechanical properties of concretes depend on the proportions of these phases.

Raman spectra of the Portland cement, gravel, sand and the concrete test specimens subjected to thermal treatment and γ-ray irradiation at different doses are presented in Fig. 1. Raman spectrum of sand shows two peaks at 413-416 and 780-782 cm^{-1} typical for α-crystobalite [5] peaks at 779, 513, 404 and 287 cm^{-1} attributed to low albite, and a weak band at 1075 cm^{-1} due to calcium carbonate. Raman spectra of gravel are characterized by vibrational bands at 520, 484, 416 and 294 cm^{-1} assigned to coesite, anorthite, cristobalite and albite respectively [5, 6]. Portland cement presents the main vibration bands for calcium carbonate phases: i) the symmetric stretching ν_1 [CO_3] 1080-1090 cm^{-1} and ii) the split in-plane bending vibrations ν_4 [CO_3] 286 cm^{-1}, the line at 521 cm^{-1} due to vibrational modes of $[AlO_4]^{5-}$ tetrahedral in C_3A, and Raman shifts at 485, 722, 987 and 1354 cm^{-1} indicating the presence of C_3A, C_2S and C_3S. The concrete shows prominent sharp peaks at 1083 and 280 cm^{-1} due to calcium carbonate, and at 402, 478 and 509 attributed to CSH and at 569 cm^{-1} due to C_2S. In fact internal deformations of the silicate tetrahedra of type ν_2 and ν_1 [SiO_4] generate bands in the regions: 300-500 cm^{-1} and 400-600 cm^{-1} respectively [7, 8].

Raman spectra of concrete subjected to thermal cycling shows two intense bands of calcium carbonate at 1086 and 278 cm^{-1}, and also appears a very weak line at 987 cm^{-1} attributed to C_2S, the characteristic bands of CSH (400-600 cm^{-1}) practically disappear [7, 8]. Carbonation in concrete is produced by the reaction of calcium hydroxide with the carbon dioxide (CO_2) present in the atmosphere in the presence of moisture. First, CO_2 reacts with the moisture to form carbonic acid, which then reacts with $Ca(OH)_2$ to form calcium carbonate ($CaCO_3$) [4].

Concrete specimens irradiated at 200, 1000 and 10000 kGy present similar Raman spectra to the non γ-ray irradiated concrete, only bands intensities were modified. An obvious modification of the concrete phase due to irradiation occurs in the concretes γ-ray irradiated at 400 and 600 kGy. At 400 kGy, Raman spectra show only the main two bands for calcium carbonate phases (1080 and 276 cm^{-1}) and the band intensity at 1080 cm^{-1} is considerably increased. At 600 kGy, calcium carbonate practically disappears, the band intensity

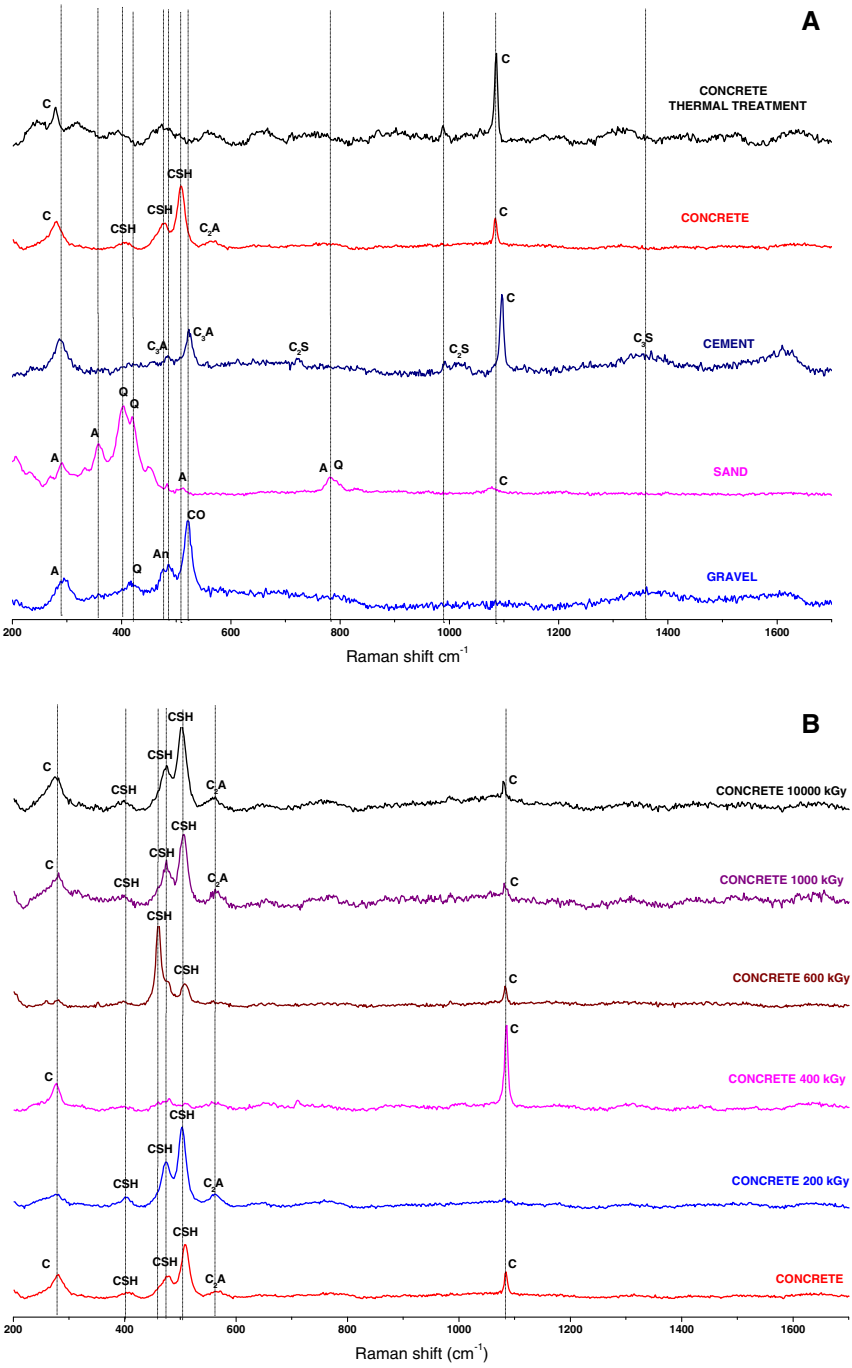

Fig. 1 Raman spectra of a) gravel, sand, cement (CPC 30RS EXTRA CEMEX), concrete and concrete heat treated, and b) concrete, and concrete specimens (γ-ray irradiated from 200 to 10000 kGy)

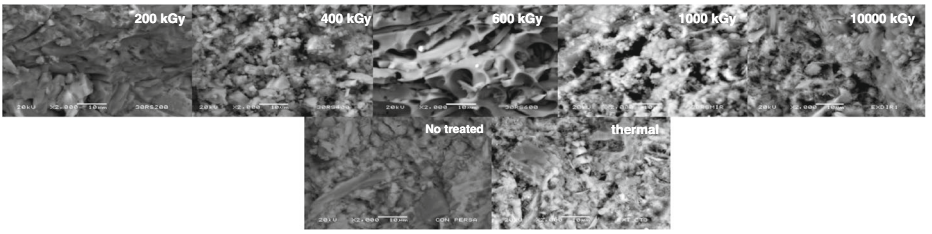

Fig. 2 Morphology of un-treated, γ-ray irradiated and heat treated concretes

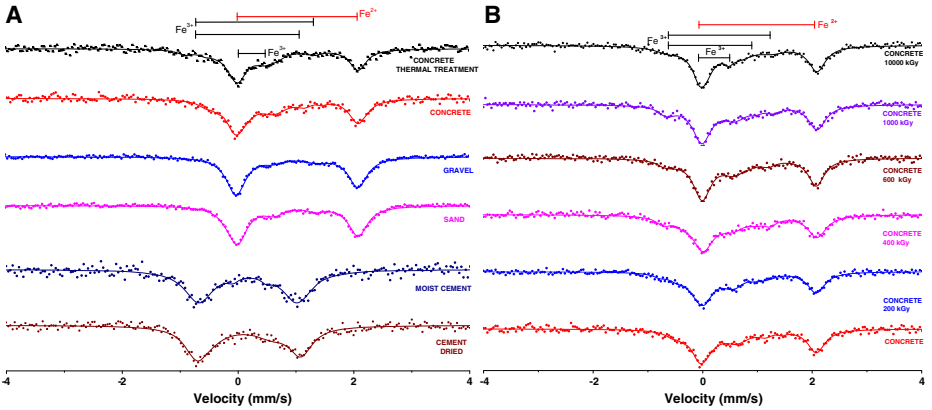

Fig. 3 Mössbauer spectra of (**a**) cements and raw materials (gravel and sand), and (**b**) γ-ray irradiated concretes

at 507 cm^{-1} decreased markedly and the broad band at 470 cm^{-1} splits into two peaks: 460 and 470 cm^{-1}. In the concrete γ-ray irradiated at 200 kGy, the band at 1083 cm^{-1} (calcium carbonate) disappears and decreased in the concretes γ-ray irradiated at 1000 and 10000 kGy. The intensities ratio of bands 470/502 is: >1 at 600 kGy and <1 for the rest of radiation doses, see Fig. 1b.

3.2 Scanning electron microscopy

Morphological changes of C-S-H (irregular or array of layers which are randomly arranged to create interlayer spaces of different shapes and sizes) [4] and ettringite (needle-shaped prismatic crystals) [4] are evident in irradiated concretes, in particular at 600 kGy (See Fig. 2). In this case concrete becomes more porous by an apparent dehydration of C-S-H and ettringite. However increasing the irradiation doses (>1000 kGy) C-S-H and preferentially ettringite rehydrate, and portlandite (large crystals with a distinctive hexagonal-prism morphology) [4] is again present in these concretes. In the case of heat treated concrete, there is no significant transformation of its morphology, with a more obvious presence of ettringite only.

3.3 Mössbauer spectroscopy

The Mössbauer spectra and parameters of the initial materials (sand, gravel, cement) and treated concretes by irradiation and heat treated are presented on Fig. 3 and Table 2 respec-

tively. The Mössbauer spectrum of cement was processed with a model of two doublets, for the gravel and the sand with three doublets, and the treated and non-treated concretes with four doublets. Mössbauer parameters show that the iron atoms in the cement is in trivalent state (Fe^{3+}), distributed in tetrahedral (T) and octahedral (O1, O2) coordination symmetries [9–11]; the gravel and sand have iron in bivalent state (Fe^{2+}) mainly, with trivalent iron (Fe^{3+}) in a low concentration, while in the concretes, the iron was found in three forms: Fe^{2+} in the tetrahedral site (T) and Fe^{3+} in the tetrathedral and octahedral sites.

According to Mössbauer parameters of the concretes (Table 2), the intensities $I_1(T)$, $I_2(O1)$, $I_3(O2)$ and $I_4(Fe^{2+})$, the isomer shifts $\delta_1(T)$, $\delta_3(O2)$ and $\delta_4(Fe^{2+})$, and the quadrupole splitting $\Delta_1(T)$, $\Delta_3(O2)$ and $\Delta_4(Fe^{2+})$ do not show significant changes as a result of the thermal or γ-ray irradiation treatment of the concretes. However both treatments cause a decrease of $\delta_2(O1)$ and $\Delta_2(O1)$; $\delta_2(O1)$ values fall from 0.6 (untreated concrete) to about 0.3 for the treated concrete while $\Delta_2(O1)$ values decrease from 1.8 (untreated concrete) to around 1.4 for the irradiated concretes and to 1.2 for the heat treated. On the other hand, $I_3(O2) > I_2(O1)$ in the untreated and treated concretes, except for the irradiated concrete at 200 kGy, in this case $I_2(O1) > I_3(O2)$. The ratio $I_3(2)/I_2(O1)$ in untreated concrete is 3.6, this ratio changes with the γ-ray irradiation and the heat treatments between 1.15 and 2, respectively.

Regarding the Mössbauer parameters of raw materials (RM), it can be noted that the values of the intensities $I_4(Fe^{2+})$ and $I_3(O2)$ of the raw materials decrease from 79 % and 94 % to 50 % and 10 % respectively in the concretes, while $I_1(T)$ value increases from 5 % in the RM to 35 % for the concretes. Considering the formulation of the concretes the intensities $I_4(Fe^{2+})$ and $I_1(T)$ of the raw materials are preserved in the concretes, not so in the case of $I_3(O2)$. The quadrupole splitting values $\Delta_1(T)$, $\Delta_2(O1)$, $\Delta_3(O2)$ and $\Delta_4(Fe^{2+})$ and the isomer shifts values $\delta_1(T)$, $\delta_3(O2)$ and $\delta_4(Fe^{2+})$ of the RM and the concretes are

Table 2 Mössbauer parameters of the initial and concretes materials (δ-Isomer Shift, $\triangle$-Quadrupole Splitting, I-Area %)

Sample	δ_1 (mm/s)	δ_2 (mm/s)	δ_3 (mm/s)	δ_4 (mm/s)	Δ_1 (mm/s)	Δ_2 (mm/s)	Δ_3 (mm/s)	Δ_4 (mm/s)	I_1 %	I_2 %	I_3 %	I_4 %
Sand	0.46	0.68		1.15	0.58	1.56		2.1	16.8	8.2		74.9
gravel	0.42	0.77		1.15	0.64	1.4		2.10	10.3	11.1		78.6
Cement	0.32		0.29		0.58		1.7		5.7		94.3	
Concrete	0.46	0.66	0.41	1.13	0.56	1.81	1.7	2.12	35.4	2.4	8.6	53.6
Concrete 200 kGy	0.34	0.38	0.33	1.16	0.66	1.49	1.98	2.05	38.2	7.6	5.9	48.3
Concrete 400 kGy	0.37	0.42	0.37	1.16	0.57	1.35	1.94	2.08	36.1	5.7	11.2	47.0
Concrete 600 kGy	0.39	0.29	0.37	1.15	0.59	1.38	1.90	2.08	35.7	4.0	8.2	52.1
Concrete 1000kGy	0.40	0.31	0.41	1.15	0.6	1.56	1.99	2.11	33.9	6.7	8.5	50.9
Concrete 10000 kGy	0.45	0.31	0.43	1.16	0.7	0.56	1.92	2.08	29.1	8.0	13.2	49.7
Thermal	0.33	0.2	0.33	1.16	0.55	1.24	2.23	2.08	36.2	6.9	7.9	49

similar. In particular the δ_2(O1) values of the RM and the untreated concrete are also similar, but they decrease in the treated concretes.

From the previous analysis, it can be inferred from relative intensities mainly that the distribution of trivalent iron in octahedral positions O1(I_2) and O2 (I_3) changes with the irradiation doses applied to concrete and with the heat treatment, and the recoil-free fractions of Fe^{2+} and Fe^{3+} do not change as a result of the transformation of the raw materials into concretes, however, part of Fe^{3+} (I_3) from cement, converts into Fe^{3+} (I_1) in concretes.

4 Discussion

One of the effects of γ-ray irradiation on materials is their thermal heating due to γ-ray absorption. If these materials contain water, the irradiation with γ-rays leads simultaneously to ionization of water and subsequent formation of H^+ ions and $OH^\bullet$ free radicals. High γ-ray doses causes the migration of most of the produced free radicals from the region of high free radicals concentration and react with the other hydrogen and molecular products to give H_2O and H_2 creating vacancies. This results in a distribution of defect environments of the host atoms residing in their original valence configurations which can also cause structural changes in the concrete and variations in their mechanical properties as the compressive strength. However the effects of gamma radiation on the mechanical properties of concrete depends on the type of cements, aggregates, mix proportions and radiation dose [12, 13].

Water exists in concretes mainly associated with C-S-H, in the following states: 1) water of constitution: interlayer hydrate water and chemically bound water, i. e., non-evaporable water, 2) Water gel includes adsorbed water and water bound by physical surfaces forces (lattice water) and 3) free water stay inside the capillary pores, not bound by surface forces [4]. The removal of free water does not cause any volume change, while the elimination of the water gel, associated with the interlayer space within the C-S-H structure, may cause shrinkage and creep of the system and it is lost by heating. Thus, evaporable water (free water and some adsorbed water) from a concrete can be removed at 100 °C, producing stresses, micro structural changes and irreversible decomposition of the concrete while non-evaporable water is lost when the concrete is heated (ignited) up to 1000 °C [4].

It has been reported that (1) γ-ray doses higher than 3000 kGy can raise the concrete temperature, leading to water liberation and radiolysis of hydration water and (2) the formation of high concentrations H^+ ions and $OH^\bullet$ free radicals at doses higher than 7000 kGy. At one of the stages of the radiolysis in concretes, the reduction of Fe^{3+}(O) to Fe^{2+}(O) may occur, considering that Fe^{3+}(O) and Fe^{2+}(O) ions are located in octahedral sites in the ferritic phase [$(CaO)_4(Al_2O_3)(Fe_2O_3)$] [12]. However, in accordance with our results, the effect of the γ-ray irradiation process on concrete caused its dehydratation at γ-ray doses less than 600 kGy, and its rehydration at γ-ray doses higher than 1000 kGy, due to a phase change of hydrates. Thus γ-ray irradiation first produces a severe drying in concrete at doses between 200 and 600 kGy, because water is released and decomposed by radiolysis to generate hydrogen and hydrogen peroxide which in turn decomposes into water and oxygen at high γ-ray doses (>1000 kGy). This dehydration/rehydration process was well established by infrared measurements not shown here [14]. On the other hand, present results do not show a reduction of Fe^{3+}(O) to Fe^{2+}(O) in our concrete, even at high γ-ray doses (10000 kGy), but only a change in the arrangement of Fe^{3+} within octahedral sites. It is possible to presume that the γ-ray heating effect may also cause a dehydration and rehydration of the

ferric hydrate phases (calcium ferrite gel or calcium sulphoferrite) present in concretes, as in the case of calcium silicate hydrate (C-S-H).

The dehydration/rehydration processes caused by the γ-ray irradiation in the concrete can produce variations in the mechanical properties depending on at the radiation dose. However, mechanical strength changes of the concrete are not produced at γ-ray doses studied in this work.

5 Conclusions

There was not a significant change in the strength properties of the prepared concrete due to the γ-ray irradiation process, neither as a result of the heat treatment. An average compression strength of 34.7 MPa was obtained for the untreated, γ-ray irradiated and thermal treated concretes.

Significant changes in the morphology and structure of the concrete γ-ray irradiated at 600 kGy are associated with modifications in the CSH phase.

Morphological changes of calcium silicate hydrates (C-S-H) and ettringite were observed by SEM images as a result of their dehydratation process from 200 to 600 kGy and rehydratation process from 1000 to 10000 kGy, caused by the radiolysis of water.

On the other hand, iron was found as TetracalciumAlumino Ferrite $4CaO\bullet Al_2O_3\bullet Fe_2O_3$ (C_4AF) in the Portland cement and a mineral of Fe^{2+} in the sand and gravel with a low content of Fe^{3+}. The latter iron species do not change while preparing the concretes or treating them either with γ-ray of heat. The major changes were observed in the ferric phase associated with the C_4AF compound that is present in the original cement, where variations of the Mössbauer hyperfine parameters of the O1 and O2 sites were detected. These changes could be associated with a dehydration and rehydration process of concretes.

References

1. Handling, conditioning and storage of spent sealed radioactive source. IAEA-TECDOC-1145, IAEA, Vienna (2000)
2. Norma Oficial Mexicana NOM-019-NUCL-1995.: Requerimientos para Bultos de Desechos Radiactivos de Nivel Bajo para su Almacenamiento Definitivo cerca de la Superficie
3. ASTM C-39: Standard Test Method for Compressive Strength of Cylindrical Concrete Specimens
4. Kumar Mehta, P., Monteiro, P.J.M. Concrete: Microstructure, Properties, and Materials McGraw-Hill Professional, 4th edn. USA (2013)
5. Ferriere, L., Koeberl, C., Reimold, W.U.: Eur. J. Mineral **21**, 20–217 (2009)
6. Freeman, J.J., Wang, A., Kuebler, K.E., Joliff, B.L., Haskin, L.A.: Can. Mineral. **46**, 1477–1500 (2008)
7. Potgieter-Vermaak, S.S., Potgieter, J.H., Van Grieken, R.: Cem. Concr. Res. **36**, 656–662 (2006)
8. Martínez-Ramírez, S., Fernández-Carrasco, L.: Raman Spectroscopy:Application to Cementitious systems. In: Construction and Building: Design, Materials and Techniques. Ed. Sophie G. Doyle, Nova Science Publishers, pp. 233–244 (2011)
9. Lilkov, V., Petrov, O., Tzvetanova, Y., Savov, P.: Constr. Build. Mater. **29**, 33–41 (2012)
10. Lilkov, V., Petrov, O., Tzvetanova, Y., Savov, P., Kadiyski, M.: J. Spectrosc. **1-9** (2013). doi:10.1155/2013/23184
11. Hassaan M.Y., Eissa N.A.: Applicatons of Mössbauer Spectroscopy in Cement Studies. International Centre for Theoretical Physics, IAEA, UNESCO **IC/86/235**, 1-51 (1986)
12. Eissa, N.A., Kany, M.S.I., Mohamed, A.S., Sallam, A.A., El Fouly, M.H.: Hyperfine Interact. **112**, 205–212 (1998)

13. Maruyaman, I., Kontani, O., Sawada, S., Sato, O., Igarashi, G.: structure-background, Takizawa, M. Concrete preparation of neutron irradiation test. In: Proceedings of the ASME 2013 Power Conference, POWER2013-98114, pp. 1-9, USA (2013)
14. González Neri, M., Monroy Guzman, F., González, R.C., Díaz, G., Ortíz Arcivar, I.J., Pérez, C.: Characterization of concretes for conditioning of spent radioactive sources. XXIII Internacional Materials Research Congress, México (2014)